Progress Towards Increased Understanding and Control of Internal Transport Barriers (ITBs) on DIII–D* EX

E.J. Doyle,[1] C.M. Greenfield,[2] J.E. Kinsey,[3] M.E. Austin,[4] L.R. Baylor,[5] K.H. Burrell,[2] T.A. Casper,[6] J.C. DeBoo,[2] D.R. Ernst,[7] P. Gohil,[2] R.J. Groebner,[2] G.L. Jackson,[2] T.C. Jernigan,[5] L.L. Lao,[2] M. Makowski,[6] G.R. McKee,[8] M. Murakami,[5] W.A Peebles,[1] R. Prater,[2] C.L. Rettig,[1] T.L. Rhodes,[1] B.W. Rice,[6] G.M. Staebler,[2] B.W. Stallard,[6] E.J. Synakowski,[7] D.M. Thomas,[2] M.R. Wade,[5] R.E. Waltz,[2] and L. Zeng[1]

[1]Dept. of Electrical Engineering and IPFR, University of California, Los Angeles, California 90095, USA. E-mail: doylej@fusion.gat.com
[2]General Atomics, P.O. Box 85608, San Diego, California 92186, USA
[3]Lehigh University, Bethlehem, Pennsylvania 18015, USA
[4]University of Texas at Austin, Austin, Texas 78712, USA
[5]Oak Ridge National Laboratory, Oak Ridge, Tennessee 37381, USA
[6]Lawrence Livermore National Laboratory, Livermore, California, 94550, USA
[7]Princeton Plasma Physics Laboratory, Princeton, New Jersey 08543, USA
[8]University of Wisconsin-Madison, Madison, Wisconsin 53706, USA

Improved theory-based understanding of ITB dynamics is needed to guide current experimental investigations and is vital for establishing a robust predictive capability for next generation devices. Similarly, ITB control capabilities are required to sustain the ITB and to realize predicted gains in fusion performance and stability limits: increasing the spatial extent of the barrier (increasing ρ_{ITB}) increases fusion performance and MHD stability limits, and results in a favorable bootstrap alignment with the total current profile, while control of gradients is required so as to avoid instabilities and disruptions. Highlights of recent progress on DIII–D towards understanding and control of ITBs include the first successful modeling of the dynamics of energy and momentum ITBs in DIII–D plasmas, use of counter-NBI (injection anti-parallel to plasma current) to produce larger ρ_{ITB} with reduced gradients, production of simultaneous ITBs in all four transport channels, and use of pellet and neon impurity injection to trigger improved confinement. These results begin to put in place validated experimental and theoretical tools for an integrated demonstration of ITB control within a time scale of a few years.

Understanding of ITB dynamics

A single physical mechanism, turbulence and transport reduction by sheared E×B flows, is thought to play an essential, though not necessarily unique, role in generating improved transport regimes observed on DIII–D and other devices, and many qualitative and quantitative tests of this model have been performed. The essential next step in testing E×B stabilization models is to replicate the observed dynamics of ITB formation. Such a test has now been performed using the GLF23 transport model to evolve temperature and velocity profiles, while self-consistently computing the effects of E×B shear flow stabilization, for discharges with negative central magnetic shear $\hat{s}$ (NCS discharges). The simulation results are in excellent agreement with the observed evolution of the experimental profiles, exhibiting step-wise ITB spatial growth at constant input power, with localized precursors to the growth events. These results indicate that the complex DIII–D ITB dynamics can be successfully replicated by a local E×B driven transport bifurcation model, further increasing confidence in our theory-based understanding of ion and momentum transport.

Considerable progress has also been made with regard to understanding electron transport. Clear electron transport barriers are observed on DIII–D in specific operating regimes, but are harder to obtain than ITBs in the ion channel, and transport in the electron channel always remains anomalous. Analysis of experimental profiles using the GKS code indicates that ∇T_e in the ITB region may be limited by marginally unstable high-wavenumber ETG-type turbulence. That ETG modes may be controlling electron transport in DIII–D NCS plasmas is also supported by the recent GLF23 modeling, which has replicated the dynamical evolution of experimental T_e profiles as well as the T_i and angular rotation profiles already mentioned. Finally, the GLF23 code will be used to reanalyze previous cases where the GKS code indicated stable ETG modes, even though χ_e was anomalous.

*Work supported by U.S. Department of Energy under Grants DE-FG03-86ER53225, DE-FG03-96ER54373, DE-FG03-97ER54415, and Contracts DE-AC03-99ER54463, DE-AC05-96OR22464, DE-AC02-76CH03073, and W-7405-ENG-48.

Control of ITB characteristics

ITB formation: With co-NBI, ITBs in the ion thermal and angular momentum transport channels can be obtained with or without NCS operation, and at injected power levels at or below 2.5 MW. For counter-NBI, however, ion ITBs only consistently form above a power threshold of ~9 MW. However, ITB formation at low power levels with counter-NBI has been recovered by pellet injection from the high field side. As regards the electron thermal and particle transport channels, localized steep ITBs are only observed with strongly reversed magnetic shear (strong NCS), and for particle transport barriers, at power levels above ~8 MW. Thus, with strong NCS and high input power, simultaneous, localized ITBs can be obtained in all four transport channels.

ITB expansion: Apart from input power density, the two major factors believed to govern the radius to which ITBs expand are the magnetic shear profile and the detailed interplay between rotational and pressure gradient terms in the expression for $\omega_{E\times B}$. Turbulence growth rates are predicted to reduce as $\hat{s}$ is reduced, making it possible for lower levels of E×B shear to suppress turbulence in NCS plasmas as compared to plasmas with positive shear. This is believed to be one reason why ρ_{ITB} is often observed to lie close to the radius of minimum q, ρ_{qmin}, in NCS plasmas. Consequently, several attempts have been made to increase ρ_{qmin} as a potential means to increase ρ_{ITB}. A ρ_{qmin} of ~0.9 has been obtained using a rapid current ramp and early high power co-NBI, but ρ_{ITB} was still limited to ~0.4–0.5. This result demonstrates that while low or negative $\hat{s}$ may facilitate ITB formation and expansion, it is not a sufficient condition. Experiments to increase ρ_{ITB} by varying the interplay between the rotational and pressure gradient terms contributing to $\omega_{E\times B}$ have proved more successful. In co-NBI discharges a null in $\omega_{E\times B}$ is often created as a result of the opposition of rotational and pressure terms in the expression for $\omega_{E\times B}$, see Fig. 1(a). With counter-NBI, the rotational and pressure terms add rather than oppose, and no null is created in $\omega_{E\times B}$, removing an impediment to the expansion of ρ_{ITB}, see Fig. 1(b). A comparison of the ITBs in co- and counter-NBI plasmas with similar input powers shows that ρ_{ITB} is indeed larger in the latter, increasing from ρ~0.4 in the co-NBI plasma to ρ~0.6 with counter-NBI. Other experimental tools are also available with which to try to expand ρ_{ITB}, in particular, neon impurity injection into NCS plasmas results in a zone of improved confinement in the outer positive shear region at 0.6<ρ<0.8. In future work we will attempt to link this latter region to transport barriers in the negative shear region, so as to form a single expanded zone of improved confinement. With the increased ECH power planned for DIII–D in 2000 (3.5 MW), we will also soon be in a position to attempt to expand ρ_{ITB} by localized ECH deposition at the foot of pre-existing ITBs.

Control of ITB gradients: as a result of broader NBI deposition, ITB gradients with counter-NBI are reduced as compared to those observed in similar co-NBI plasmas. Other potential gradient control tools, such as modulated off-axis ECH, have been identified, but have yet to be explored.

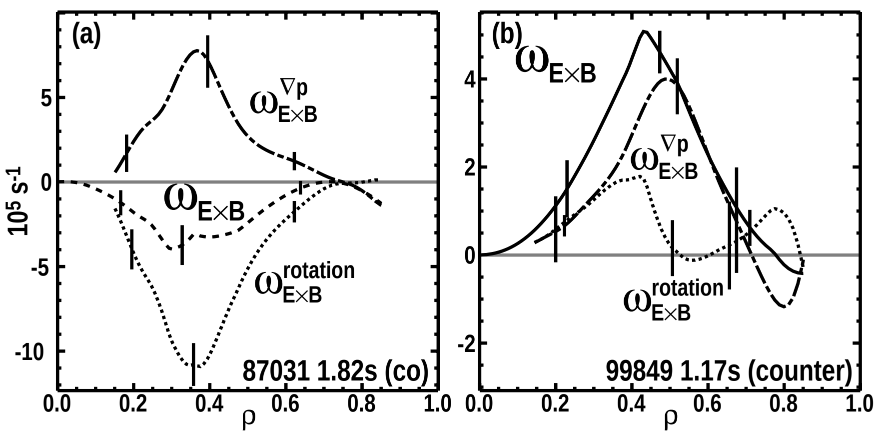

Fig. 1. Total shearing rate $\omega_{E\times B}$ and component main ion pressure gradient and rotational shearing rate terms for (a) co-NBI, and (b) counter-NBI, showing changes in the interplay between the pressure gradient and rotational terms with co- and counter-NBI.